REPORT NO.
UCB/SESM-80/06

STRUCTURAL ENGINEERING AND
STRUCTURAL MECHANICS

SEISMIC RISK ANALYSIS OF STRUCTURAL SYSTEMS

by
ARMEN DER KIUREGHIAN

Report to Sponsor:
National Science Foundation

SEPTEMBER 1980

DEPARTMENT OF CIVIL ENGINEERING
UNIVERSITY OF CALIFORNIA
BERKELEY, CALIFORNIA

SEISMIC RISK ANALYSIS OF STRUCTURAL SYSTEMS

By

Armen Der Kiureghian
Assistant Professor of Civil Engineering
University of California, Berkeley

A report on research sponsored by
the National Science Foundation

Report No. UC SESM 80-6
Division of Structural Engineering
and Structural Mechanics
Department of Civil Engineering
University of California, Berkeley

September 1980

ABSTRACT

A methodology for reliability assessment of structural systems subjected to seismic risk is developed. Based on modern concepts of structural reliability theory, structural safety against earthquakes is described through a performance function of a set of ground motion variables. A multi-variate risk analysis is then performed to compute the failure probability. The method can be applied to any type of structural system for which a performance function can be formulated. A specific application to linear structures using the response spectrum of ground motion is developed where the performance function is shown to be of quadratic form in terms of response spectral ordinates. This application is illustrated through a numerical example for a two-degree-of-freedom linear structure with multiple failure modes. The example is also used to examine the accuracy of a conventional method that uses marginal probabilities to approximate a joint distribution.

ACKNOWLEDGEMENT

This research was supported by the U.S. National Science Foundation under Grants No. ENG-7905906 and PFR-7822265. This support is gratefully acknowledged. Special thanks are due M. Moghtaderizadeh, graduate student in SESM, who carried out the numerical computations.

TABLE OF CONTENTS

INTRODUCTION

Probabilistic methods for seismic risk assessment of engineering facilities have become of increasing interest and demand in recent years. Following Cornell's original work in 1968 (4), several analytical methods for the assessment of seismic risk have been developed (e.g. 2,8,11). These methods for the most part are concerned with the risk associated with a single ground motion intensity variable (usually the peak ground acceleration), i.e. the probability that at a given site the intensity variable will exceed a specified threshold during a given interval of time. Results from such studies are often used for safety analysis of structural systems and for developing seismic design criteria for such systems. The implicit assumption in such applications is that a single ground motion intensity descriptor, such as the peak ground acceleration, is sufficient to describe the performance or safety of the structural system. Although this assumption may be appropriate for a preliminary analysis or design, it clearly is a very crude approximation for most structural systems.

Motivated by the response spectrum method of dynamic analysis (3,12), more recently, the concept of a risk-consistent response spectrum has been proposed as a method that provides a better description of structural safety (1,7,11). Such spectra are developed by using the peak response of a linear, single-degree-of-freedom oscillator as the measure of ground motion intensity and by performing a series of independent risk analyses at selected frequencies and damping ratios of the oscillator. A risk-consistent spectrum is then obtained by plotting the peak responses of the oscillator corresponding to a selected probability of exceedance. It is implicitly assumed in this approach that a structure designed on the basis of a risk-consistent response spectrum has a failure probability equal to the exceedance probability of the spectrum. However, since the risk analyses for the response spectrum ordinates at various frequencies are performed independently, they represent marginal risks and, therefore, do not include the effect of dependence (or lack of dependence) between the ordinates. The implication is that in

using such a spectrum for dynamic analysis one may be combining modal responses which do not necessarily correspond to the same earthquake. To see this more clearly observe that the peak responses of two oscillators with different characteristics and subjected to a set of earthquake motions may in general occur during different earthquakes. For example, the peak response of a high-frequency oscillator may occur during a moderate but nearby earthquake, whereas that for a low-frequency oscillator may occur during a large but distant earthquake. If the oscillators represent modes of a structure, clearly it would not be appropriate to combine the peak responses which correspond to different earthquakes. Thus, a structure designed based on a risk-consistent response spectrum may have a failure probability different from the exceedance probability associated with the spectrum.

Presented in this paper is a new methodology for reliability assessment of structural systems subjected to seismic risk. The method combines the modern concepts of structural reliability and the existing techniques of seismic risk analysis into a unified theory which, at least conceptually, can be applied to all classes of structural systems. A specific application of the theory to the class of linear structures is discussed and illustrated through an example. The example is also used to examine the accuracy of the risk-consistent response spectrum approach. A discussion on the generality of the method and its conceptual application to nonlinear structures concludes the paper.

DEVELOPMENT OF THE THEORY

Following modern concepts of structural reliability (10), let the performance of a structure subjected to earthquake induced ground motions be described through a *performance function*

$$g(Y_1, Y_2, \ldots, Y_n) \tag{1}$$

where Y_i are random variables describing the ground motion at the site of the structure resulting from a random earthquake in the seismic region surrounding the site. Let the function $g(.)$ be defined such that for any specific ground motion described by $\mathbf{y} = \{y_1, y_2, \ldots, y_n\}$, $g(\mathbf{y}) \leq 0$

implies failure and $g(\mathbf{y}) > 0$ implies survival of the structure relative to safety (i.e., maintenance of structural integrity) and/or serviceability (i.e. maintenance of structural operability). In general, the function $g(.)$ may include other random variables that describe the resistances of the structure or environmental effects other than the ground motion (i.e., other loads). For the sake of clarity, however, such variables are excluded from consideration at this time, but will be included later in this development.

The variables Y_i represent any set of descriptors of ground motion which are collectively capable of determining, through the function $g(.)$, the failure or survival of a given structure. Possible examples are ground motion parameters such as the peak acceleration, velocity, displacement, and the duration of motion, or the set of response spectral amplitudes corresponding to the modal frequencies and dampings of the structure. (The latter represent peak responses of linear, single-degree-of-freedom oscillators having the modal frequencies and dampings of the structure and subjected to the same ground motion.) Other examples are the Modified Mercalli intensity measure or energy-related ground motion intensity descriptors, such as root-mean-squares of the ground acceleration or velocity. In fact, any combination of the above ground motion descriptors is a viable set for Y_i. The number of variables, n, that are included in the performance function depends on the complexity of the structure and on the degree of sophistication or accuracy desired. Generally, a larger number of variables would allow a more realistic description of structural performance and, hence, would lead to a more accurate estimation of seismic risk.

As in structural reliability theory (10), a geometric interpretation of the preceding formulation is possible. Consider the n-dimensional space of variables Y_i. For a specific structure, i.e. a given performance function, this space is divided into two regions; a *safe region*, where $g(.)$ is positive, and an *unsafe region*, where $g(.)$ is negative. The boundary between the two regions is the *failure surface* given by

$$g(y_1, y_2, \ldots, y_n) = 0 \tag{2}$$

Figure 1 illustrates this concept for a two-dimensional case. For a random earthquake in the

seismic region, the ground motion at the site with variables Y_i registers in the n-dimensional space as an hyper-point. If the point is inside the safe region the structure survives; otherwise it fails. The seismic risk problem, thus, becomes the problem of determining the probability that during the given life of a structure an earthquake will occur with the corresponding ground motion registering a point outside the safe region. Evaluation of this probability clearly requires a multi-variate risk analysis incorporating the joint distribution of Y_i.

Information or data for direct evaluation of the joint distribution of Y_i for arbitrary sites are invariably non-existent. What may in general be available is information on the probable magnitudes and potential locations of future earthquakes in the seismic region. Therefore, it is necessary to transform such information into information on Y_i. Let each Y_i be described through an *attenuation law* of the form

$$Y_i = f_i(M,R) \tag{3}$$

where M denotes the random magnitude of the earthquake, R denotes its random distance from the site, and $f_i(.)$ denotes a deterministic function. Such laws are formulated on empirical or semi-empirical basis through regression analysis of recorded motions from past earthquakes (see, for example, Refs. 1,9,11). In formulating such laws, it is usually possible to include mean effects of regional and local geologic characteristics. However, variabilities in such effects or in the complex nature of the source mechanism usually can not be included. As a result, such regression studies invariably show large scatter of data around the mean curves. To include the effect of such variabilities, the attenuation law in Eq. 3 is augmented by a random correction factor, Z_i, yielding

$$Y_i = Z_i f_i(M,R) \tag{4}$$

where the distribution of Z_i is obtained from the residuals of regression analysis (9,11).

Substituting Eq. 4 in Eq. 1, one obtains for the performance function

$$\begin{aligned} g(Y_1, Y_2, \ldots, Y_n) &= g[Z_1 f_1(M,R),\ Z_2 f_2(M,R), \ldots,\ Z_n f_n(M,R)] \\ &= G(M,R,\mathbf{Z}) \end{aligned} \tag{5}$$

where $\mathbf{Z} = \{Z_1, Z_2, \ldots, Z_n\}$. The function $G(M,R,\mathbf{Z})$ is now the performance function given

in terms of the earthquake variables M, R, and $\mathbf{Z}$. In the space of these variables, the failure surface is given by

$$G(m,r,\mathbf{z}) = 0 \tag{6}$$

and the safe and unsafe regions are where $G(.) > 0$ and $G(.) \leqslant 0$, respectively. An earthquake in the seismic region registers as a hyper-point in this space. Again, if the point is inside the safe region the structure survives, otherwise it fails.

Using the performance function in terms of earthquake variables, the probability of failure for a random earthquake is

$$P[G(M,R,\mathbf{Z}) \leqslant 0] \tag{7}$$

Observe that computation of this probability now requires the joint distribution of M, R, and $\mathbf{Z}$. In addition, of prime interest is the probability of failure to earthquakes occurring during a given lifetime $0,t$. This will be denoted by

$$P[G(M,R,\mathbf{Z}) \leqslant 0 \ \textit{in} \ \{0,t\}] \tag{8}$$

where M, R, and $\mathbf{Z}$ are now sequences of random variables associated with random occurrences of earthquakes in time. To compute this probability, a model for the occurrence of earthquakes in time and the interrelationship between the corresponding sets of variables is required. For this purpose, the Fault-Rupture model of Der Kiureghian and Ang (8) with improvements by Der Kiureghian (5) will be used in this paper. The basic assumptions and idealizations in this model are:

1. The seismic environment in the region of the site is described through a set of faults (sources) modeled as straight-line segments situated in horizontal planes. The locations or orientations of faults in these planes are either well known or are random with uniform distribution over area sources. The depths to horizontal planes are assumed to be known.

2. An earthquake in the seismic region originates as an intermittent series of ruptures randomly occurring along a given fault or in an area source. The total rupture length, l, is given as a function of the earthquake magnitude

$$l = l(m) \tag{9}$$

The rupture may occur anywhere along the given fault or in the area source with uniform likelihood.

3. The ground motion at a site is most influenced by the closest segment of rupture to the site. Thus, the distance R in attenuation laws is taken as the shortest distance from the site to the rupture.

4. Occurrences of earthquakes in time and space are statistically independent events. The occurrences in time constitute Poisson events with ν_j denoting the mean occurrence rate in source j and $\nu = \sum_j \nu_j$ denoting the mean occurrence rate in the entire region.

5. Magnitudes of earthquakes at successive occurrences are statistically independent and identically distributed variables with the probability density function $f_M(m)$.

6. Variables Z_i at successive occurrences are statistically independent and identically distributed with the joint probability density function $f_{\mathbf{Z}}(\mathbf{z})$.

7 Variables Z_i are independent of M and R. (Note, however, that M and R are dependent, since R being the shortest distance to the rupture is a function of the rupture length and hence of magnitude.)

From the assumption of independence between the successive occurrences of R, M, and $\mathbf{Z}$ (assumptions 4, 5, and 6 above, respectively), and from the Poisson model for earthquake occurrences in time, it follows that the occurrences of events $\{G(M,R,\mathbf{Z}) \leqslant 0\}$ in time constitute a censored Poisson process with the mean occurrence rate equal to $\nu P[G(M,R,\mathbf{Z}) \leqslant 0]$, where $P[G(M,R,\mathbf{Z}) \leqslant 0]$, it is recalled, is the probability of failure to a random earthquake. From this, the lifetime probability of failure is obtained as

$$P[G(M,R,\mathbf{Z}) \leqslant 0 \text{ in } \{0,t\}] = 1-\exp\left\{-\nu t P[G(M,R,\mathbf{Z}) \leqslant 0]\right\}$$
$$\approx \nu t P[G(M,R,\mathbf{Z}) \leqslant 0] \qquad (10)$$

where the approximation is valid for small failure probabilities. The corresponding mean return period for failure events is

$$\bar{T} = \frac{1}{\nu P[G(M,R,\mathbf{Z}) \leqslant 0]} \qquad (11)$$

Observe that the preceding two quantities are both given in terms of the probability of failure to a random earthquake. To compute this probability, the total probability theorem is used to condition on all possible sources of occurrence, i.e.

$$P[G(M,R,\mathbf{Z}) \leqslant 0] = \sum_j P[G(M,R,\mathbf{Z}) \leqslant 0 \mid E_j] P[E_j] \tag{12}$$

where E_j is the event that the earthquake occurs in source j. It should be clear from the assumption 4 above that

$$P[E_j] = \frac{\nu_j}{\nu} \tag{13}$$

Thus, it is necessary to compute the conditional probability of failure to a random earthquake in source j. This probability can be obtained by further conditioning on M and $\mathbf{Z}$ and using the total probability theorem to give

$$\begin{aligned} P[G(M,R,\mathbf{Z}) \leqslant 0 \mid E_j] &= \int_{m_0}^{m_j} \int_{\mathbf{Z}} P[G(M,R,\mathbf{Z}) \leqslant 0 \mid E_j, m, \mathbf{z}] f_{\mathbf{Z}}(\mathbf{z}) f_M(m)\, d\mathbf{z}\, dm \\ &= \int_{m_0}^{m_j} \int_{\mathbf{Z}} P[G(m,R,\mathbf{z}) \leqslant 0 \mid E_j] f_{\mathbf{Z}}(\mathbf{z}) f_M(m)\, d\mathbf{z}\, dm \end{aligned} \tag{14}$$

where the probability term in the integrand is the conditional probability of failure to an earthquake of magnitude m randomly occurring in source j with $\mathbf{Z} = \mathbf{z}$. In the above equation, m_0 denotes the lower-bound magnitude of engineering interest and m_j denotes the upper-bound magnitude in source j. The integration on $\mathbf{z}$ is in general n-fold. However, since at each occurrence the variabilities in the source mechanism and the propagation paths are the same for all Y_i, it would be reasonable in most instances to assume that Z_i are functionally dependent. Then, the vector $\mathbf{Z}$ can be replaced by a single variable Z, thus reducing the n-fold integral into a single integral.

To compute the conditional probability in the right hand side of Eq. 14, the concept of a *failure distance* is introduced. Observe that for fixed m and $\mathbf{z}$ the performance function, $G(m,R,\mathbf{z})$ is in general a monotonically increasing function of R. This is because a farther earthquake with same m and $\mathbf{z}$ would invariably be less damaging. It follows, then, that for given m and $\mathbf{z}$ there could at most be one distance for which the performance function is zero.

This distance, denoted by r_f, is the failure distance and is obtained by solving for r in Eq. 6. It is useful to introduce the notation

$$r_f = \bar{G}(m, \mathbf{z}) \tag{15}$$

where $\bar{G}(.)$ denotes the solution of $G(.,r)=0$ for r. Note that r_f is a function of m and $\mathbf{z}$, in addition to being dependent on the particular form of the performance function. Clearly, an earthquake with parameters m, $\mathbf{z}$, and r_f is situated on the failure surface of the structure. For an earthquake with given m and $\mathbf{z}$, the structure will survive if R is greater than r_f, and it will fail if R is less than or equal to r_f. Thus,

$$P[G(m,R,\mathbf{z}) \leq 0 \,|\, E_j] = P[R \leq r_f | E_j] \tag{16}$$

This leads to the idea of a *failure circle* in the horizontal plane of earthquake sources underneath the site; see Fig. 2. Inside the circle is the unsafe region, i.e. a rupture in this region will result in structural failure, and outside is the safe region, i.e. a rupture in this region will not cause failure. Thus, the problem of computing the failure probability reduces to a problem of geometry; i.e., what is the probability that a line segment of known length randomly placed along a straight line or in an area will intersect the region bounded by a circle? Solutions of this problem for several idealized cases are given in Ref. 8. For the purpose of completeness, these results with some improvements are summarized in Appendix I. With the probability in Eq. 16 determined, Eq. 14 is evaluated using numerical integration. The result is then substituted in Eq. 12 and summed over all sources yielding the probability of failure to a random earthquake. The lifetime failure probability and the corresponding return period are then obtained as in Eqs. 10 and 11, respectively.

It should be pointed out that for given m and $\mathbf{z}$ Eq. 6 may not have an acceptable root for r. In that case, the performance function is always either positive or negative, in which case the probability in Eq. 16 becomes zero or one, respectively.

As was indicated before, The performance function in Eqs. 1 and 5 may include other random variables reflecting the random resistances of the structure or other loads. Let $\mathbf{X}$ denote the vector of such variables with $f_{\mathbf{X}}(\mathbf{x})$ describing the corresponding joint probability

density function. For $\mathbf{X}$ constant in time, the probability of failure to a random earthquake is obtained, using the total probability theorem, as

$$P[G(M,R,\mathbf{Z},\mathbf{X}) \leq 0] = \int_{\mathbf{X}} P[G(M,R,\mathbf{Z},\mathbf{x}) \leq 0] f_{\mathbf{X}}(\mathbf{x}) d\mathbf{x} \tag{17}$$

whereas the lifetime probability of failure is obtained as

$$\begin{aligned} P[G(M,R,\mathbf{Z},\mathbf{X}) \leq 0 \ \ in \ \{0,t\}] &= 1 - \int_{\mathbf{X}} \exp\left\{-\nu t P[G(M,R,\mathbf{Z},\mathbf{x}) \leq 0]\right\} f_{\mathbf{X}}(\mathbf{x}) d\mathbf{x} \\ &\approx \nu t P[G(M,R,\mathbf{Z},\mathbf{X}) \leq 0] \end{aligned} \tag{18}$$

where $P[G(M,R,\mathbf{Z},\mathbf{x}) \leq 0]$ is the conditional probability of failure to a random earthquake assuming $\mathbf{X} = \mathbf{x}$, and is obtained as before using the conditional failure distance

$$r_f = \bar{G}(m,\mathbf{z},\mathbf{x}) \tag{19}$$

Note that the approximation in Eq. 18 is only valid for small failure probabilities.

APPLICATION TO LINEAR STRUCTURES

Application of the above procedure to any structural system involves three distinct steps: (a) selection of a set of ground motion descriptors that adequately characterize the structural performance; (b) formulation of the performance function with due consideration to safety and serviceability requirements; and (c) determination and idealization of regional seismicity, magnitude distribution, rupture length relation, and attenuation laws for any particular region of interest. These steps indeed involve the entire field of earthquake engineering. As an example, an application to linear structures is subsequently developed.

It is well known that any peak response (e.g. displacement, acceleration, or force at a point) of a linear, multi-degree-of-freedom structure subjected to an earthquake-induced ground motion can approximately be obtained as a combination of its modal responses in terms of the response spectrum of ground motion (3,6,12). Using a recently developed formulation (6), a peak response quantity, R_{max}, can be expressed as

$$R_{max} = \left[\sum_{i=1}^{n}\sum_{j=1}^{n} \Psi_i \Psi_j \rho_{ij} S_i S_j\right]^{1/2} \tag{20}$$

where n denotes the number of dynamic modes, Ψ_i is the effective participation factor for

mode i, ρ_{ij} is the correlation coefficient between modal responses and is approximately given by

$$\rho_{ij} = \frac{2\sqrt{\zeta_i\zeta_j}\left[(\omega_i+\omega_j)^2(\zeta_i+\zeta_j) + (\omega_i^2-\omega_j^2)(\zeta_i-\zeta_j)\right]}{4(\omega_i-\omega_j)^2+(\omega_i+\omega_j)^2(\zeta_i+\zeta_j)^2} \tag{21}$$

where ω_i and ζ_i are the natural frequency and damping coefficient, respectively, of mode i, and S_i is the response spectrum ordinate associated with mode i, representing the peak response of a linear, single-degree-of-freedom oscillator of frequency ω_i and damping ζ_i subjected to the given ground motion. The effective participation factor for each particular response quantity is a function of the modal properties and masses of the structure. For example, for the displacement associated with the k-th degree of freedom $\Psi_i=\Gamma_i\phi_{ik}$, and for the force in a spring connecting the k-th and l-th degrees of of freedom $\Psi_i=\Gamma_i(\phi_{ik}-\phi_{il})k_{kl}$, where Γ_i is the conventional participation factor for mode i (3), ϕ_{ik} is the k-th element of the i-th modal vector, and k_{kl} is the spring constant. It is observed in Eq. 20 that whereas Ψ_i and ρ_{ij} are functions of the structure properties, the spectral ordinates S_i are only affected by the ground motion. This suggests selecting the ordinates of the response spectrum at the modal frequencies and dampings of the structure as the descriptor variables, Y_i, of ground motion.

To formulate the performance function, let R_0 denote the resistance of the structure in a critical response mode. Assuming that failure occurs when $R_0 \leqslant R_{\max}$, the performance function can be expressed as

$$g(R_0,S_1,S_2,\ldots,S_n) = R_0^2 - \sum_{i=1}^{n}\sum_{j=1}^{n}\Psi_i\Psi_j\rho_{ij}S_iS_j \tag{22}$$

The corresponding failure surface is, then, expressed as

$$r_0^2 - \sum_{i=1}^{n}\sum_{j=1}^{n}\Psi_i\Psi_j\rho_{ij}s_is_j = 0 \tag{23}$$

which is a quadratic hyper-surface in the n-dimensional space of s_i.

Attenuation laws relating the ordinates of a response spectrum to the earthquake magnitude and distance have been obtained from regression analysis of recorded ground motions by, among others, McGuire (11) and Trifunac (13). Lognormal distributions for Z_i are usually found to be appropriate. Although no cross-correlation studies between spectral ordinates have

been conducted, it is expected that a multi-lognormal distribution for $\mathbf{Z}$ be a good approximation. In practice, it should be reasonable enough to assume functional dependence between Z_i and use a single variable instead of a vector. For this purpose it is reasonable to let

$$Z_i = a_i Z_1^{b_i} \qquad i = 2, 3, \ldots, n \tag{24}$$

where a_i and b_i are constants determined from the known values of the mean and the variance of Z_i. With this assumption, $\mathbf{Z}$, $\mathbf{z}$ and $f_{\mathbf{Z}}(\mathbf{z})$ in Eqs. 5-19 of the preceding section can be replaced by Z_1, z and $f_{Z_1}(z)$, respectively.

MULTIPLE FAILURE MODES

A structural system may in general have a multitude of failure modes. For example, a building may be considered as failed when each floor displacement or story shear exceeds a prescribed threshold. Associated with each failure mode there is a performance function and a corresponding failure surface (of quadratic form for a linear structure) which separates the safe and unsafe regions. Clearly, the intersection of the safe regions of all failure modes is the safe region for the structure. The corresponding boundary represents the failure surface of the structure. To compute the failure probability in this case, it is only necessary to replace Eq. 19 by

$$r_f = \max_i \bar{G}_i(m, \mathbf{z}, \mathbf{x}) \tag{25}$$

where $\bar{G}_i(.)$ corresponds to the performance function for the i-th failure mode.

EXAMPLE

Consider the two-degree-of-freedom structure with rigid floors shown in Fig. 3. Suppose from safety and serviceability considerations the following are identified as possible failure modes of the structure: (a) displacement in excess of 2.5 *in.* (0.0635 *m*) at each floor level; (b) acceleration in excess of 0.6 g at the first floor and 1.0 g at the second floor levels; and (c) shear force in excess of 140 *kip.* (623 *kN*) in each story. Following the procedure described in the preceding section, the failure surface in each of these failure modes can be expressed as

$$r_0^2 - \Psi_1^2 s_1^2 - 2\rho_{12}\Psi_1\Psi_2 s_1 s_2 - \Psi_2^2 s_2^2 = 0 \qquad (26)$$

where r_0 is the corresponding threshold or resistance and Ψ_i are the modal effective participation factors. These quantities are listed in Table 1 for the assumed properties of the structure as described above and as shown in Fig.3. Since the correlation coefficient, ρ_{12}, is always between -1 and 1, it can easily be shown that the failure surface represented by Eq. 26 is an ellipse in the two-dimensional space of s_1 and s_2. By generalization, failure surfaces for an n-degree-of-freedom structure are expected to be hyper-ellipsoids in the n-dimensional space of $s_1,\ldots,s_n$. (It has not been possible to verify this for a general case, but it is expected to be true for most structures.) Some interesting properties of these ellipsoids can be studied from the two-dimensional case under consideration. It can be shown in the two-dimensional case that the principal axes of the ellipse for each failure mode make an angle $\theta = \frac{1}{2}\tan^{-1}[4\rho_{12}\Psi_1\Psi_2/(\Psi_1^2 - \Psi_2^2)]$ relative to the coordinate axes s_1 and s_2. When the correlation coefficient, ρ_{12}, is small, as it happens when the natural frequencies of the strucutre are well spaced (6), the angle θ is small (provided $\Psi_1 \neq \Psi_2$) and the principal axes of the ellipse nearly coincide with the coordinate axes. In that case, the minor axis of the ellipse, which corresponds to the nearest points on the failure surface and therefore is a critical axis, lies along the coordinate axis which is associated with the larger effective participation factor. Similarly, for an n-dimensional case, the principal axes of hyper-ellipsoids will nearly coincide with the coordinate axes when the natural frequencies of the structure are well spaced. In that case, the minor axis will correspond to the coordinate with the largest effective participation factor.

Fig. 4 illustrates six ellipses corresponding to the six failure modes of the example structure. These have been plotted using Eq. 26 and the values of r_0 and Ψ_i in Table 1. The principal axes of each ellipse are indicated in this figure by attached short line segments. In the second to fourth quadrants, the ellipses are shown by dashed lines to indicate that no failures through these quadrants are possible since S_i by definition are positive (6). It is observed in this figure that the principal axes of failure ellipses for the second story shear and the second floor acceleration are at 45 degrees and the minor and major axes are almost equal. This is

because the corresponding effective participation factors of the two (dynamic) modes happen to be identical for these responses (see Table 1). For all other failure modes the principal axes are nearly coincident with the coordinate axes because of the small correlation coefficient ($\rho_{12}=0.012$). It is also interesting to note that for displacement and base shear failures the minor axes are along s_1, reflecting the significant contribution of the fundamental mode to these responses, whereas for the first floor acceleration the minor axis is along s_2 reflecting the significance of the second (dynamic) mode to this response. The combined safe region of the structure is indicated in Fig. 4 as the shaded area. Observe that the critical failure modes that bound this region are the shear force in story 1 and the acceleration in floor 1.

The structure is assumed to be located in a seismic region as described in Fig. 5. The mean occurrence rates on the two faults are assumed to be $\nu_1=1$ and $\nu_2=2$ per year, respectively, and the corresponding upper-bound magnitudes are assumed to be $m_1=7.0$ and $m_2=8.5$ on the Richter scale. The lower-bound magnitude is assumed to be $m_0=4.0$. As is common in seismic risk analysis (4,8), the probability density function of the earthquake magnitude is specified in the form

$$f_M(m)=\frac{\beta\exp[-\beta(m-m_0)]}{1-\exp[-\beta(m_j-m_0)]} \tag{27}$$

where β is the regional seismicity parameter. For the present example, $\beta=1.5$ is assumed. For attenuation laws, the regression results of McGuire (11) were used to obtain $S_1=0.46\exp(0.82M)(R+25)^{-1.20}$ and $S_2=1.01\exp(0.51M)(R+25)^{-1.34}$, where M is in Richter scale, R is in kilometers, and S_1 and S_2 are in inches. Since these laws were developed using R as the focal distance, for consistency the rupture length l was set to zero in this example. Also, for simplicity, the random correction factors for the two attenuation laws were assumed to be identical, i.e. $Z_1=Z_2=Z$ was assumed. Using results in Ref. 11, a normal distribution for $\ln Z$ with the mean equal to zero and the standard deviation equal to 0.54 was assumed.

Fig. 6 summarizes the results of seismic risk analysis for the individual failure modes of the structure and for various ranges of the respective resistance or threshold, r_0. Results for both random attenuation (i.e., including Z) and deterministic attenuation (i.e., excluding Z) are

shown to demonstrate the significance of attenuation uncertainty. For the specific values of r_0 in Table 1, the failure probability in each individual failure mode as well as the probability of failure due to the combination of failure modes (i.e., the probability of being outside the shaded area in Fig. 4, computed using the failure distance in Eq. 25) are shown in Table 2. Observe that, for deterministic attenuation, the probability of failure due to the combination of failure modes is the same as the probability of failure in the first story shear. This is because for deterministic attenuation the largest value that S_2 can assume is 0.26 in. (corresponding to a magnitude 7 earthquake on fault 1) which is smaller than the value at which the first floor acceleration becomes a critical failure mode, see Fig. 4. For random attenuation, both the first story shear and the first floor acceleration contribute to the failure event and, as a result, the probability of failure due to the combination of failure modes is greater than that for each individual failure mode (see Table 2).

The preceding results provide a means for examining the accuracy of the risk-consistent response spectrum approach. To generate such spectra, risk estimates for the spectrum ordinates S_1 and S_2 are computed using conventional seismic risk analysis. These are shown in Fig. 7. Note that these probabilities represent marginal values. At selected risk levels, values of S_1 and S_2 are used to compute the responses of the structure using Eq. 20. The results are shown in Fig. 6 at the corresponding risk levels as open and closed circles for deterministic and random attenuation, respectively. It is remarkable that the risk-consistent spectrum method, which entirely neglects the statistical dependence (or lack of dependence) between S_1 and S_2, so closely approximates the exact risk estimates. (A similar observation was made by McGuire (11) through a different approach using a large number of simulation studies for specific two-degree-of-freedom systems.) The accuracy of the risk-consistent spectrum approach may be attributed to a high degree of statistical dependence between response spectrum ordinates of ground motion and/or to an insignificant contribution from two or more earthquakes to the total risk for each response quantity. It may also have resulted in this example from the assumption of linear dependence between Z_1 and Z_2. Clearly, additional investigation is

needed to examine the accuracy of the risk-consistent response spectrum technique for different types of structures and for different seismicity settings. Such investigation is beyond the pricipal objective of this paper and will not be pursued here.

DISCUSSION AND CONCLUSIONS

An important aspect of the proposed method for seismic risk analysis of structural systems is its generality. The method need not be restricted to any class of structures (e.g. linear) or to any specific reliability criterion (i.e. safety or serviceability). In each case one only needs to select an appropriate set of ground motion descriptor variables, Y_i, and formulate the performance function based on knowledge on structural behavior and on the reliability criterion of interest. This may not be simple for certain structural systems, such as nonlinear structures, for which the behavior under seismic loading is not easily described by a finite set of variables. However, even in such cases, crude formulations of the performance function, incorporating only the most critical elements, are possible which will lead to meaningful estimates of the seismic risk. For example, for safety analysis of ductile reinforced concrete structures, whose failures during earthquakes are usually due to low-cycle fatigue, a simple performance function in terms of the peak ground velocity or acceleration and the duration of motion may be appropriate. Clearly, as research in understanding the seismic behavior of structural systems continues, more refined performance functions can be formulated leading to more realistic estimates of seismic risk.

It should also be realized that the proposed method is not limited to the particular seismic risk model utilized in this paper. More realistic assumptions with regard to, for example, generation of earthquakes, their occurrences in time and space, and the interdependence between earthquake variables at successive occurrences can be implemented at the potential expense of increased computations.

With regard to the application to linear structures, the proposed method is quite straight forward and efficient. It is particularly useful when the structure has multiple failure modes.

One disadvantage of the method that can be pointed out is that it requires the properties of the structure, i.e. mode shapes, frequencies, etc., for computation of the seismic risk. Thus, it is more of an analysis tool than design. The risk-consistent response spectrum technique, on the other hand, is appropriate as a design tool since for any selected risk level the spectrum can be generated independently of the structural properties and then used to check the corresponding responses of any selected design structure. One should, however, keep in mind that this method disregards the statistical dependence between the spectral ordinates and as such it is only an approximate technique. Note also that this method does not provide any means for including the effect of multiple failure modes.

APPENDIX I.- EVALUATION OF EQUATION 16 FOR IDEALIZED SOURCE MODELS

The following results are based on source models developed in Ref. 8. The assumptions here, however, are somewhat less restrictive and the models provide more flexibility in idealizing a seismic region. Four source models are included: (a) well known fault; (b) area with preferred fault orientation; (c) area with unknown faults; and (d) uniform seismicity region.

Well Known Fault-- Consider a straight-line fault of length L situated at depth h and horizontal distance d from the site; see Fig. 8. Suppose that a rupture of length l is randomly placed along the fault. Assuming that the rupture has equal likelihood of being anywhere along the fault without extending beyond the known ends of the fault, the probability that it will intersect the region bounded by the failure circle is

Case i - fault extending on both sides of site, Fig. 8(a):

$$P[R \leqslant r_f | E_j] = \begin{cases} 0; & \text{if } r_f \leqslant \sqrt{h^2+d^2} \\ \dfrac{2q+l}{L-2l}; & \text{if } q \leqslant a-l \\ \dfrac{q+a}{L-l}; & \text{if } a-l \leqslant q \leqslant b-l \\ 1; & \text{if } b-l \leqslant q \end{cases} \tag{28}$$

Case ii - fault extending on one side of site, Fig. 8(b):

$$P[R \leqslant r_f | E_j] = \begin{cases} 0; & \text{if } r_f \leqslant \sqrt{h^2+d^2+a^2} \\ \dfrac{q-a}{L-l}; & \text{if } q \leqslant b-l \\ 1; & \text{if } b-l \leqslant q \end{cases} \tag{29}$$

where a and b are as shown in Fig. 8 and $q=\sqrt{r_f^2-h^2-d^2}$. It is noted that these solutions include an improvement over those in Ref. 8 which were based on the assumption that the center of rupture could occur anywhere along the fault, thus permitting half the rupture length to extend beyond the known ends of the fault.

Area with Known Fault Orientation - Consider a seismically active area A situated at depth h underneath the site; see Fig. 9(a). Suppose the exact locations of faults in this area are not known, but for geological reasons it is believed that ruptures may occur along a preferred

orientation, say parallel to axis $o-o$ in Fig. 9(a). The probability that the rupture will intersect the failure circle can be evaluated from the preceding results by considering a set of imaginary faults parallel to axis $o-o$, as shown in Fig. 9(b). Assuming that the rupture may occur anywhere in the area with uniform likelihood, the mean occurrence rate of earthquakes on each imaginary fault is obtained as a fraction of the total occurrence rate (in area A) proportional to the "tributary" area of the fault as described in Fig. 9(b).

Area with Unknown Faults - Consider a seismically active area A situated at depth h underneath the site; see Fig. 10(a). Suppose the locations as well as orientations of faults in this area are unknown. Consider a small elemental area, ΔA, at a horizontal distance d from the site. Assume that an earthquake in ΔA originates as a rupture extending on both sides along a random orientation such that the ends of the rupture are randomly placed on a circle of radius $l/2$; see Fig. 10(a). The probability that the rupture will intersect the region bounded by the failure circle is clearly a function of the relative positions of the two circles. Assuming a uniform distribution over 0 to 2π for the random orientation of rupture, one obtains (8)

$$P[R \leqslant r_f | E_j] = \begin{cases} 0; & \text{if } r_f \leqslant h \text{ or } \sqrt{r_f^2-h^2}+l/2 \leqslant d \\ \dfrac{\gamma}{\pi}; & \text{if } \sqrt{r_f^2-h^2+l^2/4} \leqslant d \leqslant \sqrt{r_f^2-h^2}+l/2 \\ \dfrac{\alpha}{\pi}; & \text{if } \sqrt{r_f^2-h^2} \leqslant d \leqslant \sqrt{r_f^2-h^2+l^2/4} \\ 1; & \text{if } d \leqslant \sqrt{r_f^2-h^2} \end{cases} \tag{30}$$

where $\gamma = \cos^{-1}[(h^2+d^2+l^2/4-r_f^2)/dl]$ and $\alpha = \sin^{-1}(\sqrt{r_f^2-h^2}/d)$. Since the solution is independent of the angular position of ΔA relative to the site, ΔA may be assumed in the form of an annular area. Thus, a seismic area of general shape can be decomposed into elemental areas in the form shown in Fig. 10(b). Assuming uniform seismicity in area A, the mean occurrence rate for each elemental source is obtained as a fraction of the total mean occurrence rate in proportion to its "tributary" area, see Fig. 10(b).

Uniform Seismicity Region - In some cases it is reasonable to assume that the entire seismic region surrounding the site has uniform seismicity. Consider a circular region of radius d at depth h underneath the site, see Fig. 11. Assuming uniform seismicity, the probability that

the rupture will intersect the region bounded by the failure circle is

$$P[R \leqslant r_f | E_j] = \begin{cases} 0; & \text{if } r_f \leqslant h \\ p^2 + \dfrac{2l}{\pi d} p; & \text{if } \sqrt{r_f^2 - h^2} + l/2 \leqslant d \\ 1 + \dfrac{2}{\pi}[p\sqrt{1-p^2} - \cos^{-1} p]; & \text{if } \sqrt{r_f^2 - h^2} \leqslant d \leqslant \sqrt{r_f^2 - h^2} + l/2 \\ 1; & \text{if } d \leqslant \sqrt{r_f^2 - h^2} \end{cases} \tag{31}$$

where $p = \sqrt{r_f^2 - h^2}/d$. The above result was obtained in Ref. 8 based on the assumption that the rupture occurs along a preferred orientation. However, it can easily be shown that the same result also applies if the rupture is assumed to have a random orientation with a uniform distribution over 0 to 2π.

APPENDIX II.- REFERENCES

[1] Anderson, J.G., and Trifunac, M.D., "Uniform Risk Functionals which Describe Strong Ground Motion," *Bulletin of the Seismological Society of America,* Vol. 68, No. 1, February, 1978, pp. 205-218.

[2] Blume, J.A., and Kiremidjian, A.S., "Probabilistic Procedures for Peak Ground Motions," *Journal of the Structural Division,* ASCE, Vol. 105, No. ST11, Proc. Paper 14976, November, 1979, pp. 2293-2311.

[3] Clough, R.W., and Penzien, J., *Dynamics of Structures,* McGraw-Hill, New York, N.Y., 1975.

[4] Cornell, C.A., "Engineering Seismic Risk Analysis," *Bulletin of the Seismological Society of America,* Vol. 58, No. 5, October, 1968, pp. 1583-1606.

[5] Der Kiureghian, A., "Seismic Risk Analysis Including Attenuation Uncertainty," *Proceedings,* U.S.-Southeast Asia Symposium on Engineering for Natural Hazards Protection, Manila, Philippines, 1977, Edited by A. H-S. Ang, Department of Civil Engineering, University of Illinois, Urbana, IL., 1978, pp. 99-109.

[6] Der Kiureghian, A., "A Response Spectrum Method for Random Vibrations," *Report No. UCB/EERC-80/15,* Earthquake Engineering Research Center, University of California, Berkeley, CA., June, 1980.

[7] Der Kiureghian, A., and Ang, A. H-S., "Risk-Consistent Earthquake Response Spectra," *Proceedings,* Sixth World Conference on Earthquake Engineering, New Delhi, India, January, 1977.

[8] Der Kiureghian, A., and Ang A. H-S., "A Fault-Rupture Model for Seismic Risk Analysis," *Bulletin of the Seismological Society of America,* Vol. 67, No. 4, August, 1977, pp. 1173-1194.

[9] Donovan, N.C., "A Statistical Evaluation of Strong Motion Data Including the February 9, 1971 San Fernando Earthquake," *Proceedings,* Fifth World Conference on Earthquake Engineering, Rome, Italy, June, 1973.

[10] Hasofer, A.M., and Lind, N.C., "Exact and Invariant Second-Moment Code Format," *Journal of the Engineering Mechanics Division,* ASCE, Vol. 100, No. EM1, Proc. Paper 10376, February, 1974, pp. 111-121.

[11] McGuire, R.K., "Seismic Structural Response Risk Analysis, Incorporating Peak Response Regressions on Earthquake Magnitude and Distance," Ph.D. Thesis, Department of Civil Engineering, Massachusetts Institute of Technology, Cambridge, MA., September, 1974.

[12] Newmark, N.M., and Rosenblueth, E., *Fundamentals of Earthquake Engineering,* Prentice-Hall, Inc., Englewood Cliffs, N.J., 1971.

[13] Trifunac, M.D., "Forecasting the Spectral Amplitudes of Strong Earthquake Ground Motion," *Proceedings,* Sixth World Conference on Earthquake Engineering, New Delhi, India, January, 1977.

APPENDIX III.- NOTATION

The following symbols are used in this paper:

A	source area;
a,b,d,h,q	distance terms;
a_i,b_i	constants;
E_j	the event that an earthquake occurs on source j;
$f_i(M,R)$	a function of M and R;
$f_M(m)$	probability density function of M;
$f_{\mathbf{Z}}(\mathbf{z})$	joint probability density function of $\mathbf{Z}$;
$f_{\mathbf{X}}(\mathbf{x})$	joint probability density function of $\mathbf{X}$;
$g(.)$	performance function in terms of ground motion variables;
$G(.)$	performance function in terms of earthquake variables;
$\overline{G}(.)$	solution of $G(.,r)=0$ for r;
k_{kl}	spring constant;
l	rupture length;
L	fault length;
m,M	deterministic and random values of earthquake magnitude;
m_0	lower-bound magnitude;
m_j	upper-bound magnitude for source j;
n	number of ground motion variables included in g(.);
p	probability constant;
$P(.)$	probability;
r,R	deterministic and random values of earthquake distance;
r_0,R_0	deterministic and random values of structure resistance or threshold;
r_f	failure distance;
$R_{\max}$	maximum response;
s_i,S_i	deterministic and random values of spectral ordinate for mode i;
t	time;
$\overline{T}$	mean return period for failure event;
$\mathbf{x},\mathbf{X}$	deterministic and random vectors of structure variables;
$\mathbf{y},\mathbf{Y}$	deterministic and random vectors of ground motion variables;
y_i,Y_i	elements of $\mathbf{y}$ and $\mathbf{Y}$;
$\mathbf{z},\mathbf{Z}$	deterministic and random vectors of attenuation correction factors;
z_i,Z_i	elements of $\mathbf{z}$ and $\mathbf{Z}$;
α,γ	angles for computation of probability;
β	seismicity parameter;
ΔA	elemental source area;
ζ_i	damping coefficient for mode i;
θ	angle between principal axes of ellipse and coordinate axes;
ν	mean occurrence rate of earthquakes in entire seismic region;
ν_j	mean occurrence rate of earthquakes in source j;
ρ_{ij}	correlation coefficient between responses in modes i and j;
Ψ_i	effective participation factor for mode i; and
ω_i	natural circular frequency for mode i.

Table 1. Effective Participation Factors and Resistances of Example Structure

Failure Mode	Resistance or Threshold, r_0	Effect. Part. Factors	
		Ψ_1	Ψ_2
Displacement, *in.*			
Floor 1	2.5	0.724	0.276
Floor 2	2.5	1.171	−0.171
Acceleration, *g.*			
Floor 1	0.6	0.296	0.775
Floor 2	1.0	0.479	−0.479
Shear Force, *kip.*			
Story 1	140	72.3	27.6
Story 2	140	44.7	−44.7

Note: 1 in. = 0.0254 m; 1 kip. = 4.45 kN.

Table 2. Estimated Probabilities for Example Structure

Failure Mode	Probability of Failure in 1 Year	
	Determ. Attenuation	Random Attenuation
Displacement		
Floor 1	0.0	0.091×10^{-2}
Floor 2	0.466×10^{-3}	0.482×10^{-2}
Acceleration		
Floor 1	0.826×10^{-3}	0.709×10^{-2}
Floor 2	0.569×10^{-3}	0.526×10^{-2}
Shear Force		
Story 1	0.900×10^{-3}	0.649×10^{-2}
Story 2	0.0	0.134×10^{-2}
All Modes	0.900×10^{-3}	0.749×10^{-2}

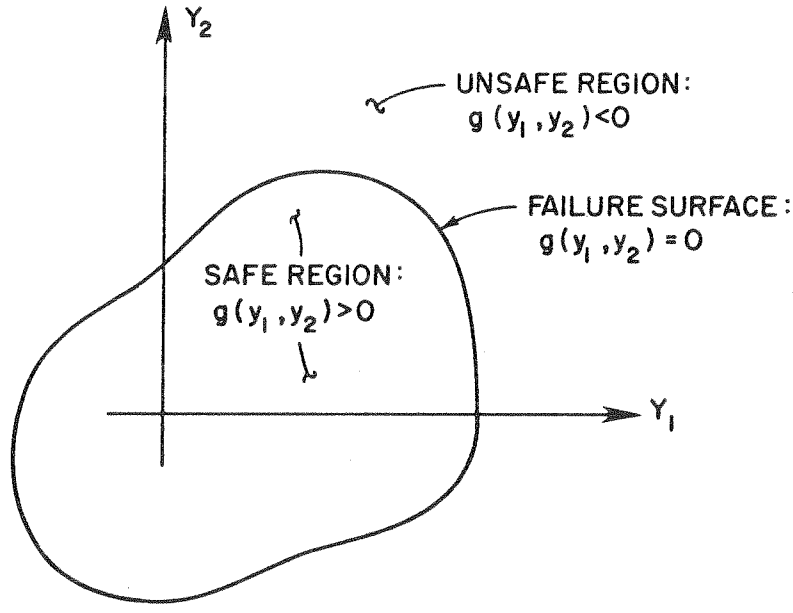

FIG. 1.- Geometric Description of Structural Safety; Two-Dimensional Case

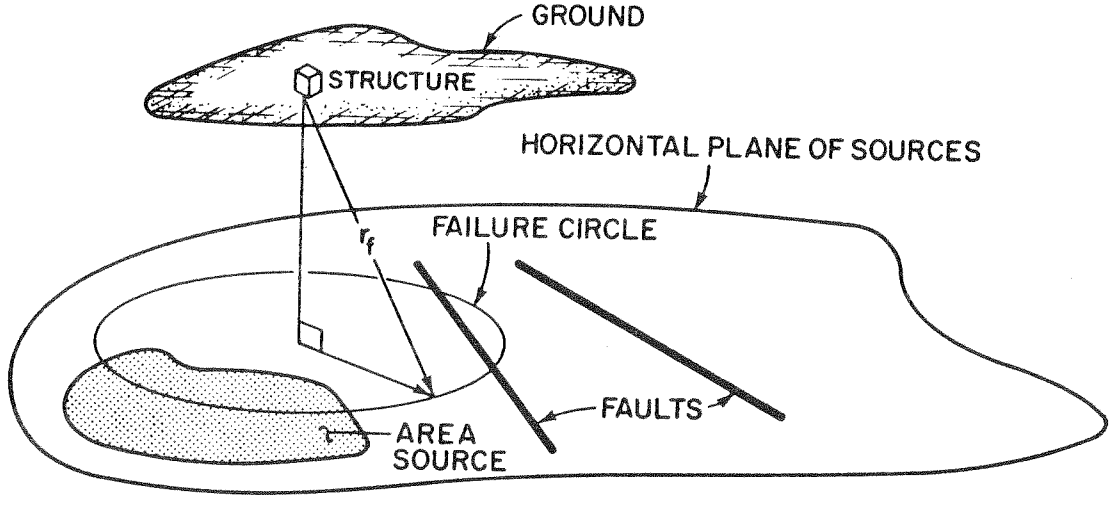

FIG. 2.- Illustration of Failure Distance, r_f, and Failure Circle

FLOOR MASS : $m = 0.24 \quad ks^2/in \quad (42050\ kg)$
STORY STIFFNESS : $k = 100 \quad k/in \quad (17520\ KN/m)$
NATURAL FREQUENCIES: $\omega_1 = 12.51, \omega_2 = 32.90\ rad/s$
MODAL DAMPING COEFFS. : $\zeta_1 = \zeta_2 = 0.05$
MODAL CROSS-CORRELATION COEFF. : $\rho_{12} = \rho_{21} = 0.012$

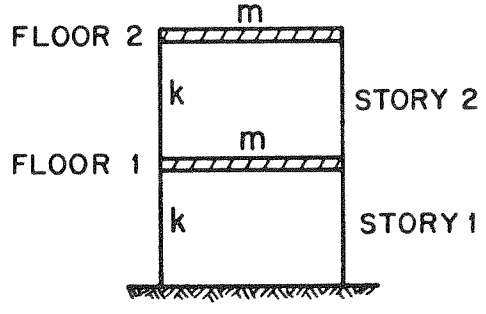

FIG. 3.- Example Structure

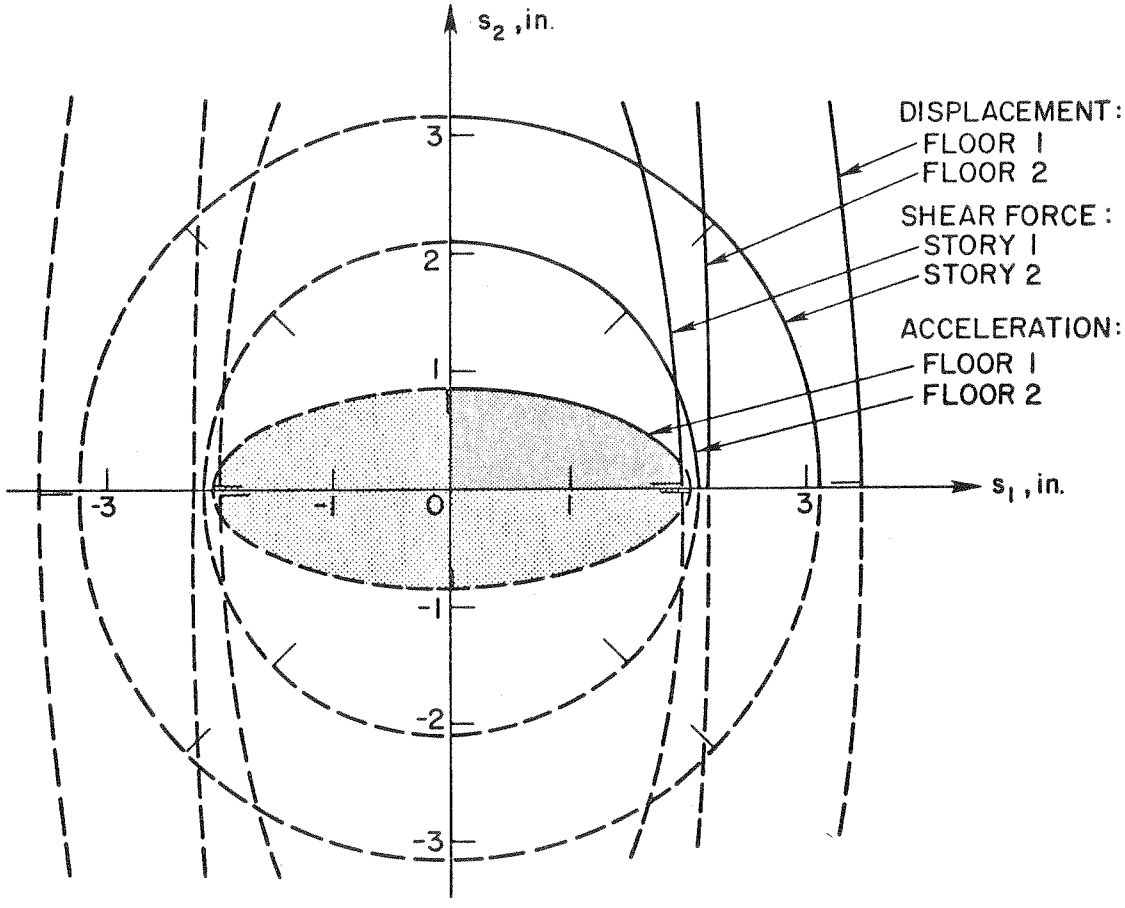

FIG. 4.- Failure Surfaces for Example Structure

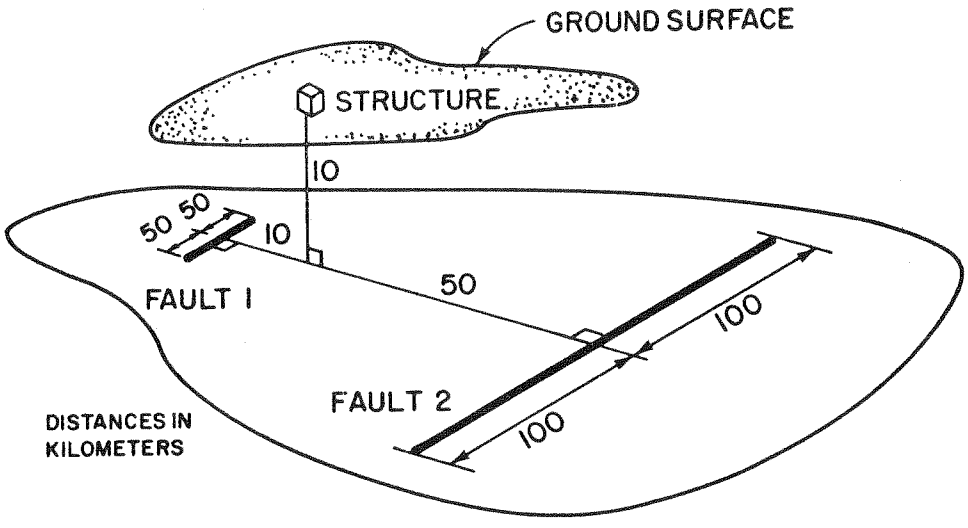

FIG. 5.- Seismicity Description for Example Structure

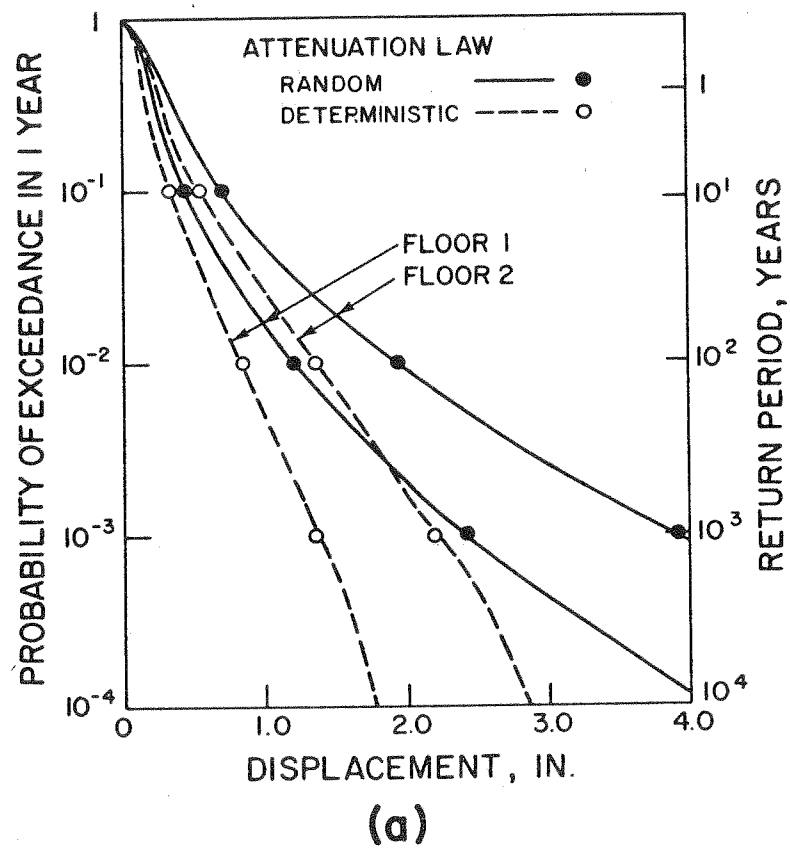

FIG. 6.- Exceedance Probabilities for Individual Failure Modes

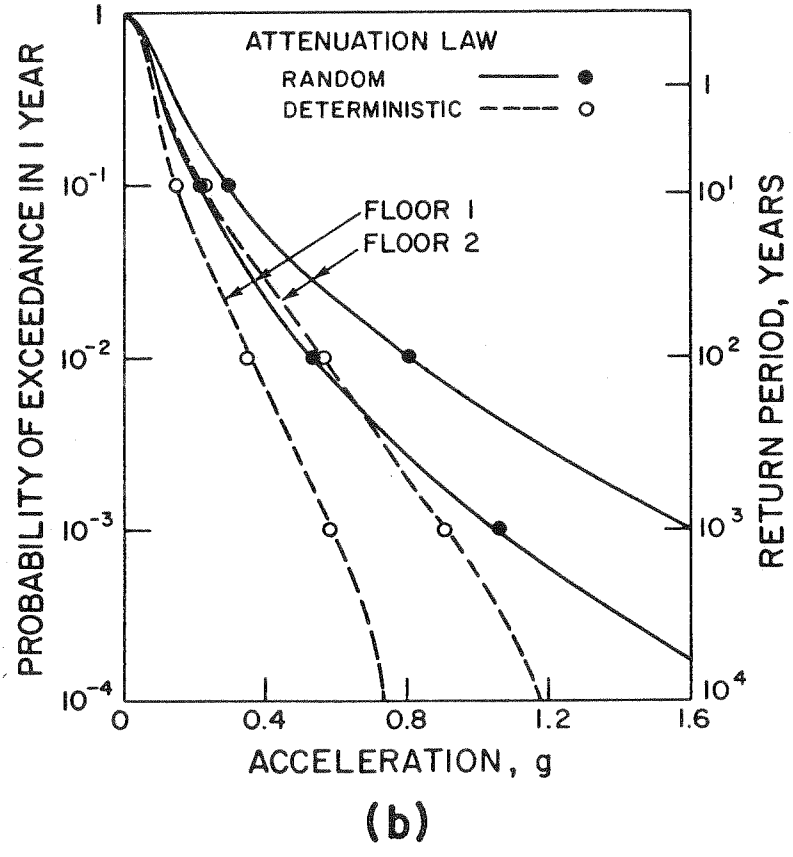

FIG. 6.- Continued

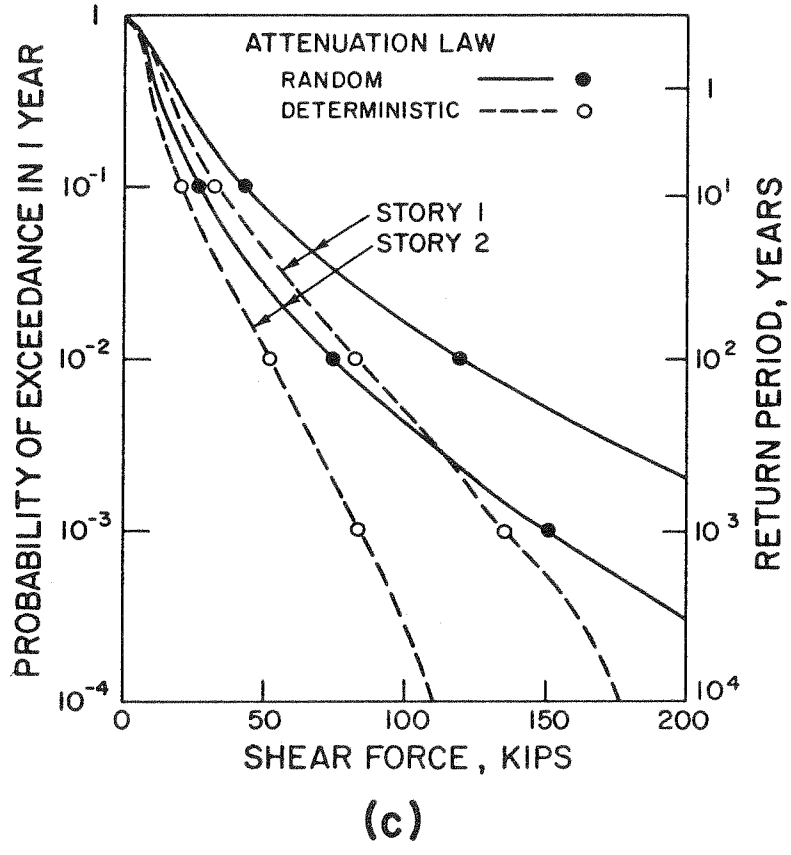

FIG. 6.- Continued

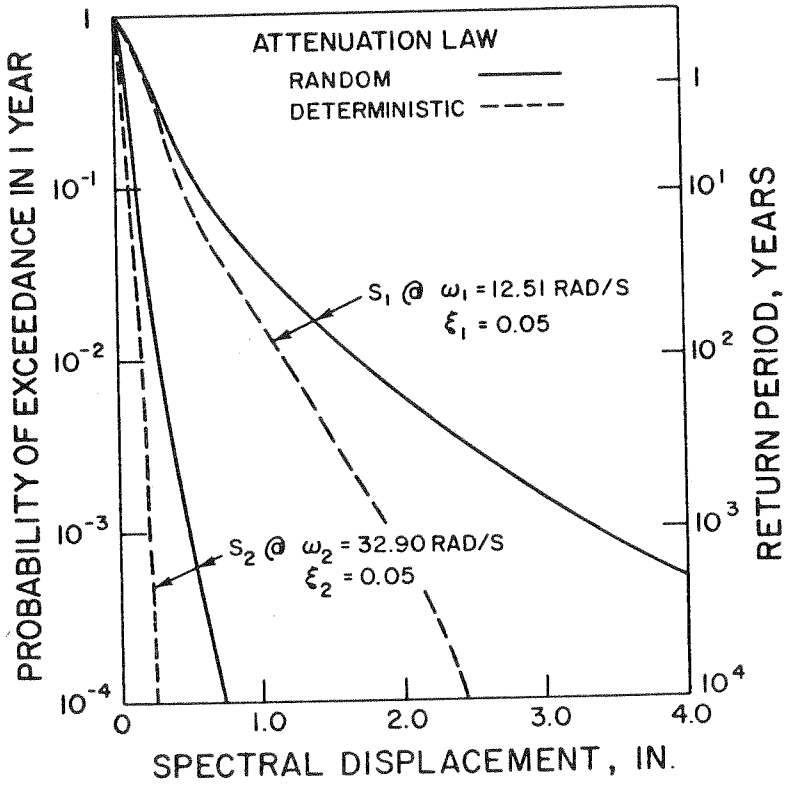

FIG. 7.- Marginal Exceedance Probabilities of Spectral Ordinates

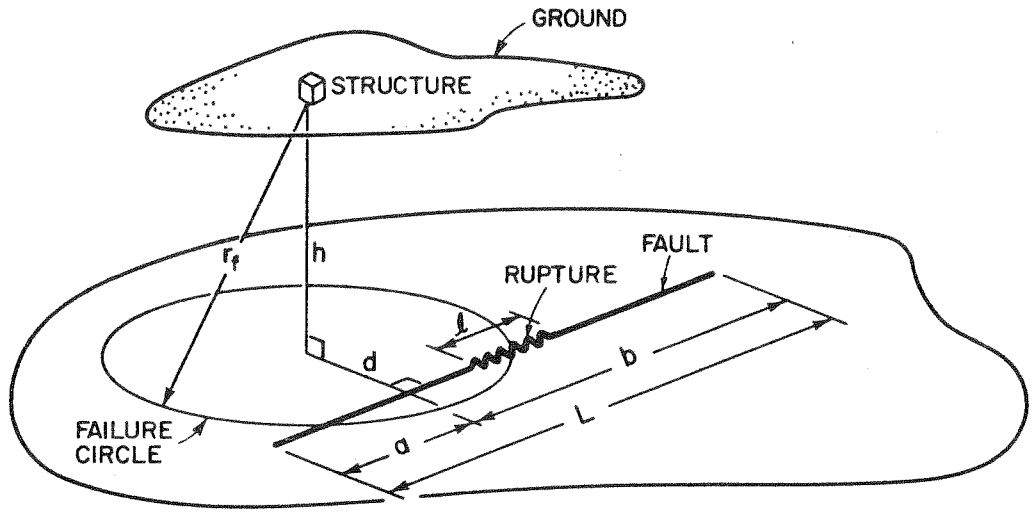

CASE - i

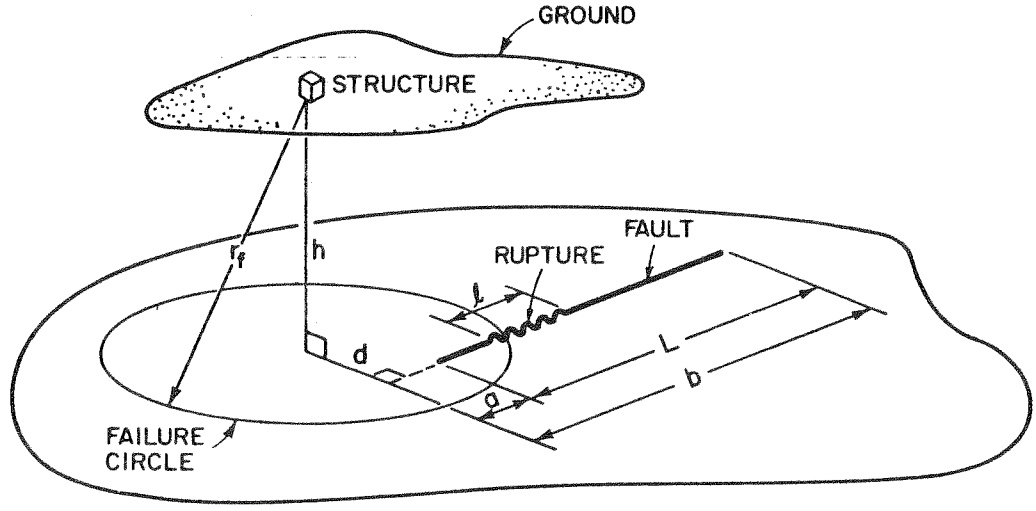

CASE - ii

FIG. 8.- Model for Well Known Fault

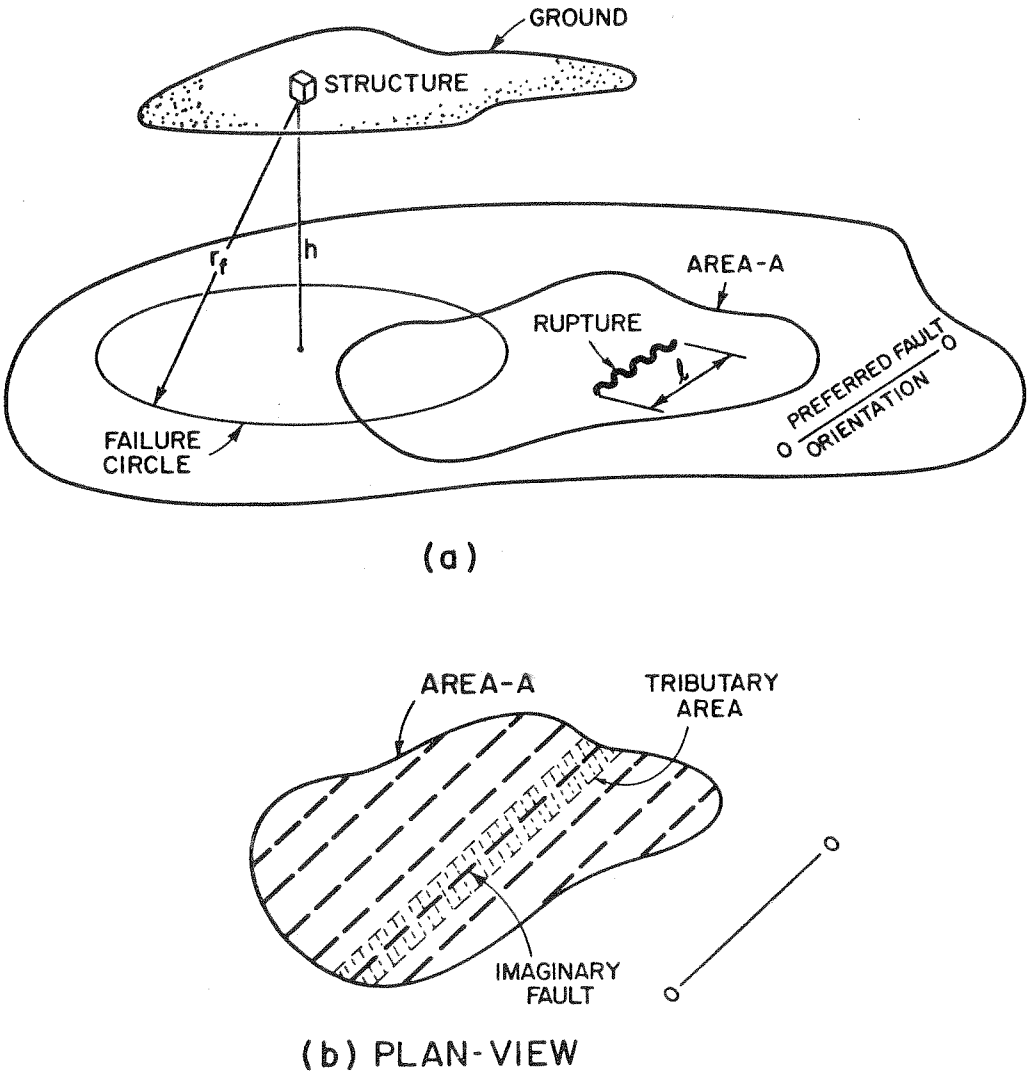

FIG. 9.- Model for Area with Preferred Fault Orientation

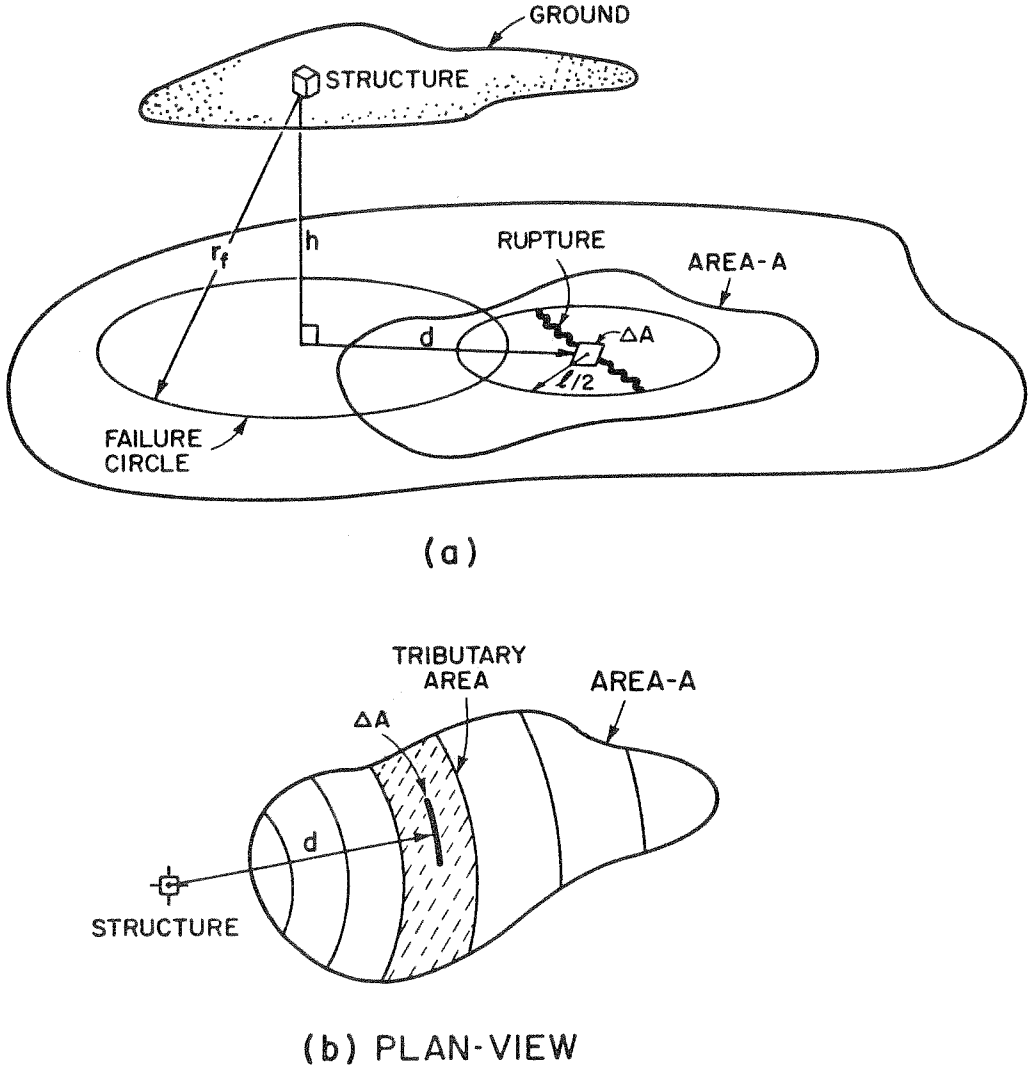

FIG. 10.- Model for Area with Unknown Faults

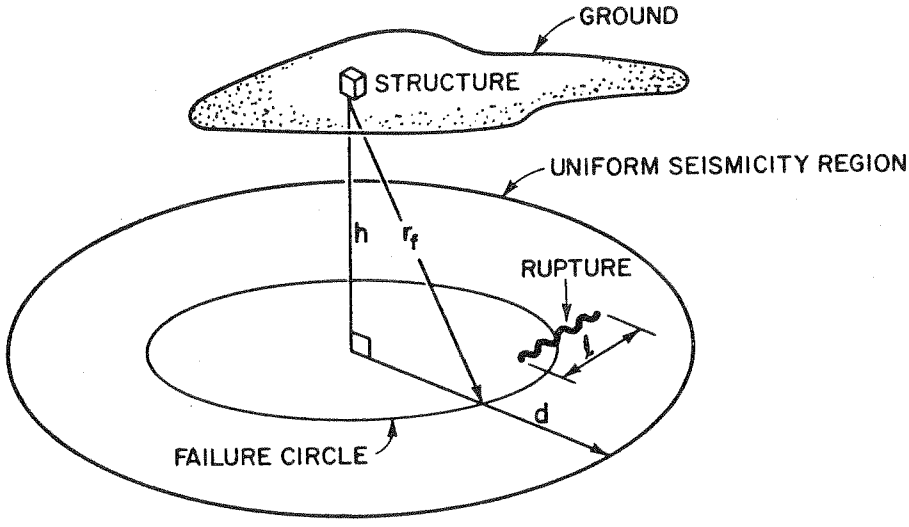

FIG. 11.- Model for Uniform Seismicity